Polymer Bulletin (2021) 78:5303–5314
https://doi.org/10.1007/s00289-020-03381-3

ORIGINAL PAPER

Investigation of poly(α-methyl styrene) tacticity synthesized by photo-polymerization

Mohammad Reza Jozaghkar[1] · Farshid Ziaee[1] · Amir Sepehrian Azar[2]

Received: 22 April 2020 / Revised: 11 September 2020 / Accepted: 23 September 2020 /
Published online: 30 September 2020

Abstract

In this work, poly(α-methyl styrene) (PAS) was synthesized by free radical photo-polymerization. The tacticity and microstructure of PAS were studied by ^{13}C nuclear magnetic resonance spectroscopy (^{13}C NMR). Assignments of all stereo sequences were carried out at pentad and hexad levels of quaternary aliphatic, quaternary aromatic, and methylene carbons using ^{13}C NMR in deuterated chloroform at 20 °C and 50 °C, respectively. It was found that by increasing the NMR acquisition temperature, higher resolution and higher splitting of the peaks were achieved for all mentioned carbons. Bernoullian and first-order Markov statistics were used for all carbons and the results were compared with experimental data by statistical method. It was shown that Bernoullian statics model fit slightly better than first-order Markov statics model for the assigned sequences. The results indicated that corresponding values of probability (P_m) was equal to 0.234, suggesting that the racemic addition was almost higher than the meso-one. The effect of the deuterated solvent on the peak resolution and the splitting of syndiotactic and isotactic sequences was investigated by replacing deuterated tetrahydrofuran with deuterated chloroform. It was observed that the peak resolution and the splitting in deuterated chloroform are much more than deuterated tetrahydrofuran.

Keywords Poly(α-methyl styrene) · NMR · Tacticity · Photo-polymerization · Microstructure

✉ Farshid Ziaee
f.ziaee@ippi.ac.ir

[1] Iran Polymer and Petrochemical Institute, P. O. Box: 14965/115, Tehran, Iran

[2] Department of Chemistry, Islamic Azad University, Ahar Branch, Ahar, Iran

Introduction

In the last decades, α-methyl styrene has been extensively interested by researchers in the blending modification, adhesives formulation, and paper coating due to its low cost and withstanding performance [1–3]. Poly(α-methyl styrene) (PAS) is one of the most promising target capsule materials in inertial confinement fusion because of its appropriate thermal degradable [4]. In addition, PAS is used for enhancing the HDT, glass temperature and mechanical properties of PVC [5].

Homopolymerization of α-methyl styrene usually carried out via ionic polymerization [6, 7]. The free-radical polymerization of α-methyl styrene is slow and predominantly yields low molecular weight due to the low ceiling temperature ($T_c = 61$ °C). The ceiling temperature is related to the strong steric repulsions between substituents in consecutive monomer units in the polymer backbone [8, 9]. Thereupon, the bulk and the solution free radical polymerization of α-methyl styrene gives the polymer with low conversion and molecular weight. In order to minimize these problems, researchers proposed an emulsion technique to synthesize high molecular weight PAS [10–12]. However, the emulsion polymerization provides the heterogeneous reactions which afford the presence of impurities in the polymer. These disadvantages could be overcome through the radiation polymerization [13, 14]. Garrett and coworkers [15] report an ESR study of free radicals formed in irradiated PAS by gamma radiation. An electron beam lithographic study of PAS and PAS-Maleic anhydride copolymer was studied by Sharma et al. [16]

Knowledge of polymer microstructures and molecular dynamic motion is crucial to acquire information concerning the relation between structure and properties as well as development industries. It is well known that NMR is one of the best analytical methods by which to attain information on the chemical structure. ^{13}C NMR has prepared stereochemical information on a large number of polymers [17, 18]. Heatley and his coworkers [19, 20] have investigated ^{13}C NMR spectra for several vinyl polymers such as isotactic and atactic polystyrenes. Using ^{13}C NMR, qualitative and quantitative analysis of tacticity can be implemented. Ziaee et al. [22] have studied the effect of temperature on the tacticity of bulk thermal polymerized polystyrene.

Many authors have investigated the stereochemical configuration of PAS by means of ^{1}H NMR. Because of three different configurations, the methyl protons of PAS are split into three peaks [23, 24]. Brownstein et al. [24] assigned these three methyl peaks to isotactic, heterotactic, and syndiotactic triads. The ^{13}C NMR of polystyrene and PAS was investigated by Inoue et al. [25]. They reported that the spectra split related to a triad, tetrad, and partially pentad placements. Comparison between ^{13}C NMR and ^{1}H NMR spectra affirmed the effect of nuclear Overhauser on the relative intensities of the peaks assigned to chemically equivalent carbons except for stereochemical configuration [26–28].

This study is designed to investigate PAS tacticity synthesized by photopolymerization at room temperature. Analysis of all stereo sequences at pentad and hexad levels of the quaternary type of aliphatic, aromatic and methylene carbon was carried out using ^{13}C NMR in different acquisition temperature. Finally, the effect of deuterated solvent on the tacticity of PAS is observed.

Experimental

Material

The α-methyl styrene (containing 4-tert-butylpyrocatechol) was supplied from Merck, Germany. Purification of the monomer was performed by vacuum distillation. Benzophenone (≥ 99%) was purchased from Sigma-Aldrich and was used as received.

Polymerization

The polymerization of α-methyl styrene was carried out by photo-polymerization using ultraviolet light with a wavelength of 254 nm at 20 °C under vacuum condition. For this purpose, after purification, the photo-initiator (BP) and monomer were injected into Pyrex glass ampoules and degassing was performed under vacuum to remove impurities such as oxygen. Then, the solution with low conversion was precipitated into methanol for removing unreacted monomers. The precipitated polymer was dried in a vacuum oven at 40 °C for 24 h.

Characterization

All NMR experiments performed in this work were carried out on a Bruker Avance 400 MHz NMR spectrometer (DMX-400, Germany). The polymer solution were prepared by dissolving 20 mg PAS in 0.5 ml of deuterated solvents. The acquisition temperature set at 20 and 50 °C. The pulse width was 90°, relaxation delay time, 2 s, acquisition time, 1.37 s, number of scans, 20,000, and data points, 64 K.

The molecular weight of PAS was determined by GPC in THF using Agilent 110 (USA). The system was calibrated with narrow molecular weight polystyrene standards ranging from 200 to 10^6 g/mol.

Results and discussion

In order to microstructure study and sequence determination, the polymer chain length must be long enough. Consequently, the GPC analysis was used to investigate the molecular weight of PAS. According to the GPC results, the number average molecular weight and the weight average molecular weight was equal to 2.25×10^4 g/mol and 4.85×10^4 g/mol, respectively.

^{13}C NMR of PAS

In ^{13}C NMR spectrum, each peak can be correlated to a specific sequence with a special chemical shift. Figure 1 demonstrates these chemical shifts attributed to the α-methyl carbon, methylene carbon, quaternary aliphatic carbon, quaternary aromatic C_1 carbon, C_2, C_3 and C_4 carbons. These carbon atoms are surrounded

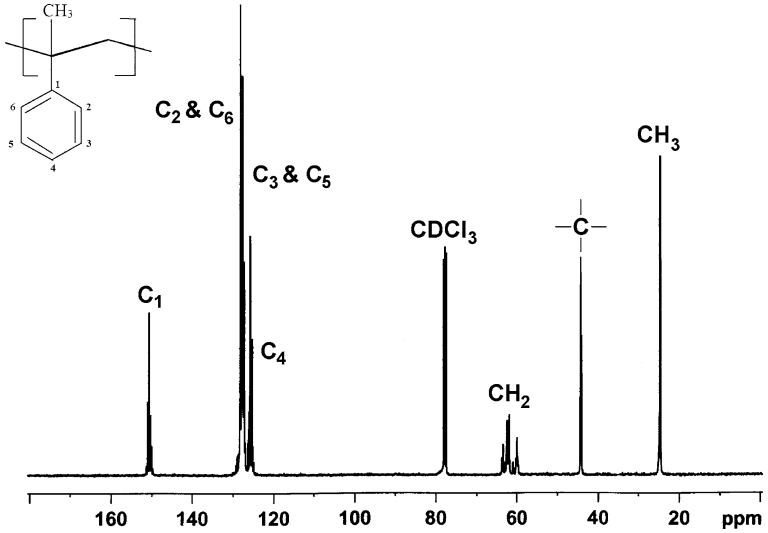

Fig. 1 ^{13}C NMR spectrum of synthesized PAS in $CDCl_3$ at 20 °C

by different isomers in the sequences. Thereupon, the neighbor carbon atoms affect each other. In this work, the study of stereospecificity was carried out on the methylene, quaternary aliphatic, quaternary aromatic and C_1 carbons. These assignments were adapted from the work of Elgert et al. [29].

Expanded ^{13}CNMR of quaternary aliphatic carbon

The quaternary aliphatic carbon of PAS is asymmetric and susceptible to the monomer insertion along the molecular chains. Furthermore, the resonance of this carbon represents distinct chemical shifts because of the microstructure. Figure 2a and b shows ^{13}C NMR spectrum of the quaternary aliphatic carbon in $CDCl_3$ at 20 and 50 °C, respectively. As it is seen from Fig. 2a, the quaternary aliphatic carbon split into 6 pentad sequences. The upfield region is rich in isotactic sequences, while the downfield region is rich in syndiotactic ones. In other words, the peaks with assignment number of 1, 2, and 3 are syndiotactic, 4 and 5 are atactic, and 6 is isotactic parts of chain. The experimental data was tested for Bernoullian and first-order Markov statics models of chain propagation and the results are shown in Table 1 and 2. As evident in Fig. 2b, by increasing the NMR acquisition temperature, higher resolution and higher splitting of the peaks are achieved. The upfield region is rich in isotactic and the downfield region is rich in syndiotactic. In the isotactic section, the number of peaks is higher at 50 °C than 20 °C, hence in this section, the heptad sequence is calculated. In statistical subject, probability of meso-(P_m) and racemic (P_r) sequences are defined by Eqs. (1) and (2), respectively. The mm, mr, and rr triad sequences have isotactic, atactic and syndiotactic parts of chain, respectively.

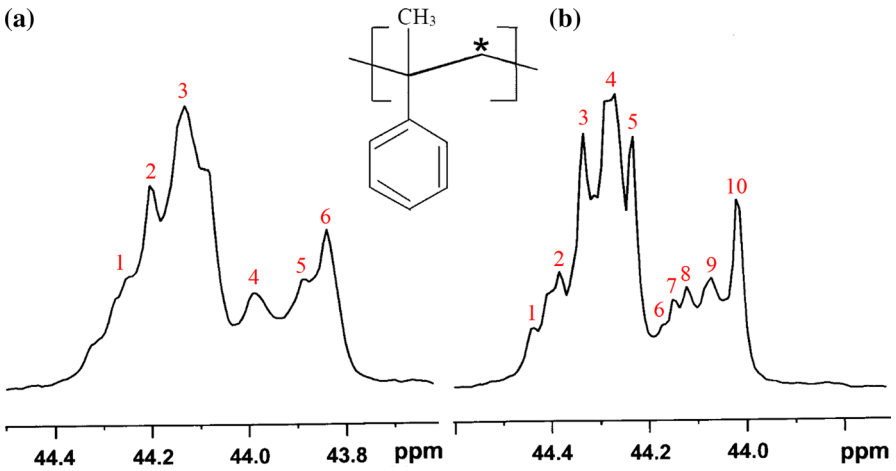

Fig. 2 Quaternary aliphatic ^{13}C NMR spectrum of PAS in $CDCl_3$ at (**a**) 20 °C and (**b**) 50 °C

Table 1 Normalized pentad sequences of quaternary aliphatic carbon, calculated Bernoullian and first-order Markov statistics in $CDCl_3$ at 20 °C

Peak no	Pentad microstructure	Chemical shift	Obs	Cal[a]	Cal[b]
1	mrrm	44.25	0.1180	0.0321	0.0244
2	mrrr	44.2	0.1491	0.2103	0.1558
3	rrrr	44.13	0.4070	0.3442	0.5386
4	rmrr + mmrm	43.98	0.1088	0.2303	0.0904
5	mmrr + rmrm	43.87	0.0735	0.1284	0.1212
6	mm	43.82	0.1436	0.0547	0.0696

[a]Bernoullian statistic equation, average sum square difference: 6.79×10^{-3}

[b]First-order Markov statistic equation, average sum square difference: 7.60×10^{-3}

$$P_m = (2\mathrm{mm} + \mathrm{mr})/2 \tag{1}$$

$$P_\mathrm{r} = (2\mathrm{rr} + \mathrm{mr})/2 \tag{2}$$

The relations between pentad, triad, and diad are attained by Eqs. (3–5) which finally enable to determine the probability of meso-sequences.

$$\mathrm{mm} = \mathrm{mmmm} + \mathrm{mmmr} + \mathrm{rmmr} \tag{3}$$

$$\mathrm{mr} = \mathrm{mmrm} + \mathrm{mmrr} + \mathrm{rmrm} + \mathrm{rmrr} \tag{4}$$

$$\mathrm{rr} = \mathrm{mrrm} + \mathrm{mrrr} + \mathrm{rrrr} \tag{5}$$

Table 2 Normalized pentad sequences of quaternary aliphatic carbon, calculated Bernoullian, and first-order Markov statistics in $CDCl_3$ at 50 °C

Peak no	Pentad microstructure	Chemical shift	Obs	Cal[a]	Cal[b]
1	mrrm	44.44	0.0391	0.0329	0.0096
2	mrrr	44.38	0.0942	0.2111	0.1410
3	rrrr	44.33	0.2662	0.3450	0.5238
4	rmrr + mmrm	44.26	0.1600	0.2307	0.0756
5	mmrr + rmrm	44.22	0.1261	0.1292	0.1064
6	rrmmrr	44.18	0.0268	0.0196	0.0169
7	mrmmrr + mrmmrm	44.15	0.0369	0.0140	0.0050
8	rmmmrr	44.12	0.0536	0.0123	0.0234
9	mmmmrr + rmmmrm + mmmmrm	44.08	0.0980	0.0016	0.0447
10	mmmmmm + mmmmmr + rmmmmr	44.01	0.0991	0.0036	0.0536

[a]Bernoullian statistic equation, average sum square difference: 4.56×10^{-2}

[b]First-order Markov statistic equation, average sum square difference: 8.38×10^{-2}

By integrating sequences areas in Fig. 2 and using Eqs. (1–5) the calculated value of P_m for all samples is equal to 0.234, indicating that synthesis PAS samples have some deviation from the ideal random case ($P_m = 0.5$) and the degree of racemic addition is constantly higher than the meso-addition. This could be related to the stereohindrance of pendant group which tend to stay away from each other and form racemic sequences [30]. However, stereoregularity of chains can be changed by increasing the polymerization temperature and variation of solvent polarity. It is encouraging to compare this finding with that found by Inoue and coworkers [25]. They reported that P_m was, respectively, equal to 0.325 and 0.125 for PAS synthesized via anionic polymerization at −78 °C and cationic polymerization at −50 °C. The value of P_m in these three polymerization methods (< 0.5) suggests that for PAS the racemic addition is almost higher than the meso-one. Therefore, due to the fact that the photo-polymerization at ambient temperature is more straightforward than the anionic and cationic polymerization, this method is recommended for the synthesis of PAS.

In accordance with Bernoullian and first-order Markov statistical model, the polymeric chain formation could be predicted. In first-order Markov model, the new monomer is added to the prior sequence which governs its configuration. first-order Markov probability is given by Eqs. 6 and 7 [22, 31].

$$P_{m/r} = 1 - P_{m/m} = \mathrm{mr}/\left(2\mathrm{mm} + \mathrm{mr}\right) \tag{6}$$

$$P_{r/m} = 1 - P_{r/r} = \mathrm{mr}/\left(2\mathrm{rr} + \mathrm{mr}\right) \tag{7}$$

$P_{m/r}$ designates that meso-diad effects the next diad situation as a racemic diad. For instance, Bernoullian and first-order Markov statistics for mrrmm are calculated as $2P_m{}^3P_r{}^3$ and $2P_m\ P_{m/r}\ P_{r/m}\ P_{m/m}\ P_{m/r}\ P_{r/r}$, respectively [31, 32]. By using sum of squared difference between two models and experimental data, adjustment

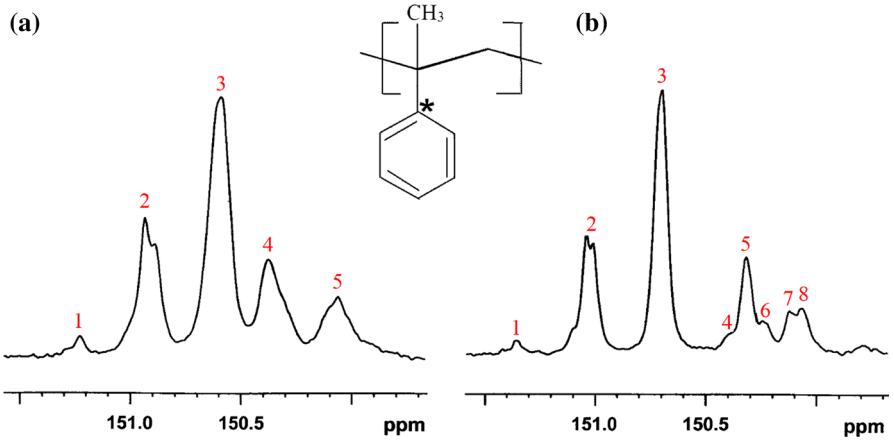

Fig. 3 Quaternary aromatic carbon ^{13}CNMR spectrums of PAS in $CDCl_3$ at (**a**) 20 °C and (**b**) 50 °C

Table 3 Normalized pentad sequences of quaternary aromatic carbon, calculated Bernoullian and first-order Markov statistics in $CDCl_3$ at 20 °C

Peak no	Pentad microstructure	Chemical shift	Obs	Cal[a]	Cal[b]
1	mrrm	151.22	0.0314	0.0322	0.0274
2	mrrr + rrrr	150.90	0.2136	0.5546	0.6821
3	mmrm + rmrr	150.60	0.4332	0.2300	0.0937
4	rmrm + mmrr	150.38	0.1775	0.1285	0.1242
5	mm	150.08	0.1443	0.0547	0.0726

[a]Bernoullian statistic equation, average sum square difference: 3.36×10^{-2}

[b]First-order Markov statistic equation, average sum square difference: 6.85×10^{-2}

of Bernoullian and first-order Markov models can be comprised for all the carbons. According to the tables, for all carbons, Bernoullian statics model can predict formation of monomers in polymer propagation more effectively.

Expanded ^{13}C NMR of quaternary aromatic carbon

^{13}C NMR spectrum of quaternary aromatic carbon in $CDCl_3$ at 20 and 50 °C is shown in Fig. 3a and b, respectively. The quaternary aromatic carbon of PAS is symmetric with different stereospecificity. As it can be seen from Fig. 3a, quaternary aromatic carbon split into 6 pentad sequences. The upfield region in the quaternary aromatic carbon of PAS is rich in isotactic sequences and the downfield region is rich in syndiotactic ones. The peak with assignment number of 1 and 2 are syndiotactic, 3 and 4 are atactic, and 5 is isotactic [33]. Normalized data for the pentad sequences at 20 and 50 °C are presented in Tables 3 and 4, respectively. It can be seen from Fig. 3b that an increase in NMR acquisition temperature, led to an enhancement of peak number from 5 to 8. The upfield region is rich in isotactic and

Table 4 Normalized pentad sequences of quaternary aromatic carbon, calculated Bernoullian and first-order Markov statistics in $CDCl_3$ at 50 °C

Peak no	Pentad microstructure	Chemical shift	Obs	Cal[a]	Cal[b]
1	mrrm	151.46	0.0274	0.0334	0.0095
2	mrrr + rrrr	151.05	0.2140	0.5559	0.6646
3	rmrr	150.70	0.4120	0.2117	0.0623
4	mmrm	150.40	0.0277	0.0210	0.0132
5	rmrm	150.30	0.1247	0.0655	0.0084
6	mmrr	150.23	0.0430	0.0655	0.0979
7	rmmr	150.12	0.0470	0.0230	0.0321
8	mmmr + mmmm	150.07	0.1042	0.0240	0.1120

[a]Bernoullian statistic equation, average sum square difference: 1.68×10^{-1}

[b]First-order Markov statistic equation, average sum square difference: 3.42×10^{-1}

the downfield region is rich in syndiotactic. Also, the overlapping is reduced and the atactic and isotactic sequences split more separately. The sum squared difference between observed and calculated data are highlighted in Tables 3 and 4. The results showed that Bernoullian propagation is fitted pretty well by experimental results.

Expanded ^{13}C NMR of methylene carbon

Figure 4a and b represents ^{13}C NMR spectrum of the methylene carbon (a symmetric carbon) in $CDCl_3$ at 20 and 50 °C, respectively. According to Fig. 4a, methylene carbon split into 11 hexad sequences. As it can be seen from Fig. 4b, by increasing the NMR acquisition temperature, higher resolution and higher splitting of the peaks are attained. Normalized data for the pentad sequences at 20 and 50 °C along with the sum squared difference between observed and calculated data are shown in Tables 5 and 6, respectively. It is found that the measured data is well consistent with calculated values based on Bernoullian statistics.

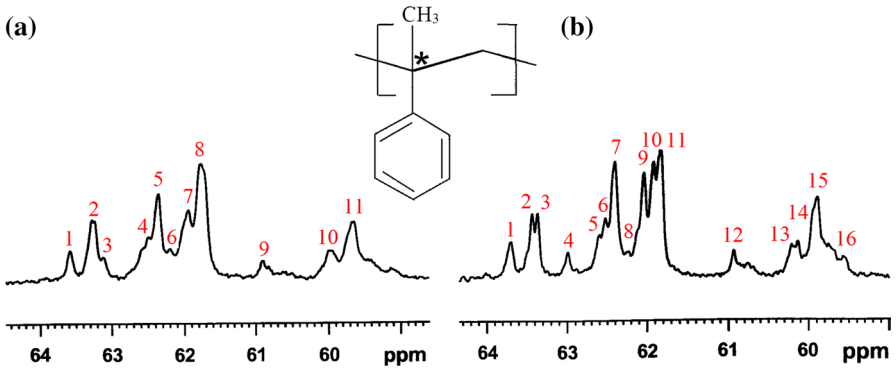

Fig. 4 Methylene carbon ^{13}CNMR spectrum of PAS in $CDCl_3$ at (**a**) 20 °C and (**b**) 50 °C

Table 5 Normalized hexad sequences of the methylene carbon, calculated Bernoullian and first-order Markov statistics in $CDCl_3$ at 20 °C

Peak no	Hexad microstructure	Chemical shift	Obs	Cal[a]	Cal[b]
1	mrmrm	63.60	0.0375	0.0080	0.0044
2	rrmrm	63.28	0.0955	0.0492	0.0115
3	rrmrr	63.10	0.0230	0.0805	0.0315
4	mmmrr + mmmrm	62.50	0.0696	0.0195	0.0720
5	rmmrr + rmmrm	62.38	0.1393	0.0642	0.0473
6	rrrrm	62.19	0.1273	0.1611	0.1287
7	rrrrr + mrrrm	61.90	0.2144	0.2883	0.4736
8	mmm + mrm	60.70	0.0551	0.0547	0.0588
9	rmrrm	60.90	0.0597	0.0492	0.0110
10	rmrrr + mmrrr	59.98	0.1585	0.2103	0.1451
11	mmrrm	59.65	0.0201	0.0150	0.0156

[a]Bernoullian statistic equation, average sum square difference: 2.39×10^{-2}

[b]Firt-order Markov statistic equation, average sum square difference: 8.64×10^{-2}

Table 6 Normalized hexad sequences of the methylene carbon, calculated Bernoullian and first-order Markov statistics in $CDCl_3$ at 50 °C

Peak no	Hexad microstructure	Chemical shift	Obs	Cal[a]	Cal[b]
1	mrmrm	63.70	0.0404	0.0075	0.0320
2	rrmrm	63.45	0.0515	0.0492	0.0102
3	rrmrr	63.35	0.0440	0.0805	0.0302
4	mmmrr	63.00	0.0286	0.0151	0.0627
5	mmmrm	62.60	0.0377	0.0046	0.0108
6	rmmrr	62.50	0.0432	0.0492	0.0409
7	rmmrm	62.40	0.1321	0.0151	0.0079
8	rrrm	62.22	0.1231	0.1612	0.1274
9	rrrrr	62.05	0.0836	0.2637	0.4640
10	mrrrm	61.90	0.1329	0.0246	0.0111
11	mmm	61.80	0.0300	0.0128	0.0156
12	mrm	60.90	0.0188	0.0419	0.0447
13	rmrrm	60.20	0.0547	0.0492	0.0102
14	rmrrr	60.17	0.1206	0.1612	0.0577
15	mmrrr	59.87	0.0381	0.0492	0.0890
16	mmrrm	59.59	0.0207	0.0150	0.0144

[a]Bernoullian statistic equation, average sum square difference: 6.57×10^{-2}

[b]First-order Markov statistic equation, average sum square difference: 16.70×10^{-2}

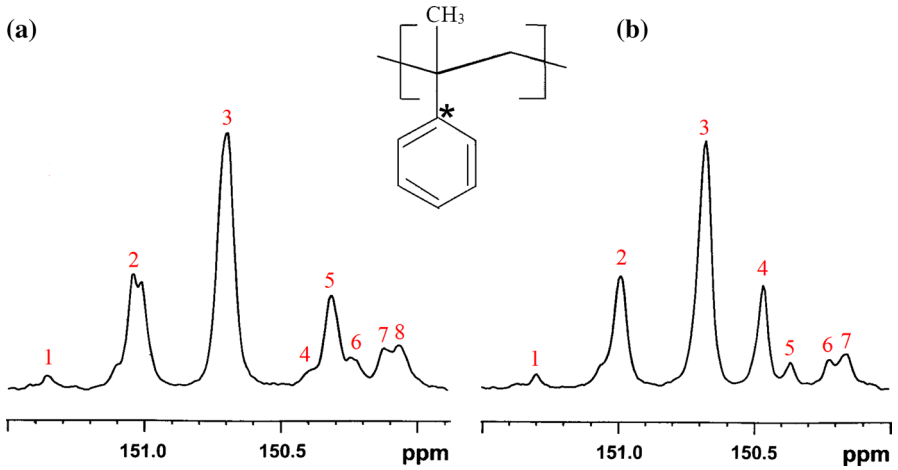

Fig. 5 Quaternary aromatic carbon ^{13}CNMR spectrum of PAS in (**a**) $CDCl_3$ and (**b**) THF-d_8 at 50 °C

Table 7 Normalized pentad sequences of the quaternary aliphatic carbon, calculated Bernoullian and first-order Markov statistics in THF-d_8 at 50 °C

Peak No	Pentad microstructure	Chemical shift	Obs	Cal[a]	Cal[b]
1	mrrm	151.30	0.0360	0.0321	0.0102
2	mrrr + rrrr	151.00	0.2271	0.5546	0.6646
3	rmrr	150.67	0.4156	0.2104	0.0623
4	mmrm + rmrm	150.47	0.1465	0.0840	0.0216
5	mmrr	150.38	0.0403	0.0642	0.0982
6	rmmr	150.22	0.0401	0.0321	0.0216
7	mmmr + mmmm	150.16	0.0944	0.0226	0.1216

[a]Bernoullian statistic equation, average sum square difference: 1.59×10^{-1}

[b]First-order Markov statistic equation, average sum square difference: 3.37×10^{-1}

Effect of THF-d_8 solvent

Several parameters can influence the degree of splitting by solvent such as relaxation time, viscosity and solubility. It is worth noting that by increasing relaxation time, higher resolution, and higher peak splitting are achieved. The same phenomenon happened by reducing solvent viscosity and increasing solubility. Figure 5 a and b shows the comparison ^{13}C NMR spectrum of the quaternary aromatic carbon of PAS in $CDCl_3$ and THF-d_8, respectively. As can be seen, contrary to the splitting of the quaternary aromatic carbon in THF-d_8, in $CDCl_3$ at the syndiotactic section, the peak with assignment number of 2 split into two sequences. Furthermore, peak resolution and the splitting in deuterated chloroform is much more than deuterated tetrahydrofuran. These results are contrary to a similar study on the polystyrene by Ziaee et al. [30] which have reported that splitting of the methylene carbon in

THF-d_8 is higher in the syndiotactic sequences. However, in this study, it can be concluded that methylene carbon has better splitting in $CDCl_3$ in all isotactic, syndiotactic and atactic sequences than THF-d_8. Table 7 shows normalized data for the pentad sequences in THF-d_8 at 50 °C. It is suggested that the measured results are in good agreement with Bernoullian statistics values.

Conclusion

The aim of the present research was to synthesize PAS by free radical photo-polymerization and investigate the tacticity and microstructure of PAS using ^{13}C NMR in different temperatures and solvents. The sequences assignments were performed at pentad and hexad levels of quaternary aliphatic, quaternary aromatic and methylene carbons. The results highlight the importance of acquisition temperature on the resolution and the splitting of the sequences. The increase in acquisition temperature led to an enhancement of resolution and number of peaks. Comparison between experimental data and calculated one by Bernoullian and first-order Markov statistics models revealed that Bernoullian statistics fit better than first-order Markov statistics for the assigned carbons. The probability of meso-addition for PAS was equal to 0.234, indicating a deviation from the random ideal case and a higher degree of racemic addition. A comparison between deuterated solvent showed that the peak resolution and the splitting of syndiotactic and isotactic sequences is $CDCl_3$ is much more than THF-d_8.

References

1. Zimmel JM, Mansour AS, Juers S, Axer V, Holtin U, Nahkala AR, Fuller HB Co, (2019) Hot melt adhesive composition for bonding packs of metal containers. US Patent 10,351,298
2. Chambers T, Goodyear Tire and Rubber Co, (1974) Adhesive composition containing an aba block copolymer, poly alpha-methyl styrene and a tackifying resin. US Patent 3,784,587
3. Hu S, Sun W, Fu J, Zhang L, Fan Q, Zhang Z, Wu W, Tang Y (2017) Reactive molecular dynamics simulations on the thermal decomposition of poly alpha-methyl styrene. J Mol Model 23(6):179
4. Zhang Z, Chen S, Zhang J (2012) A study on properties of poly (vinyl chloride)/poly (α-methylstyrene-acrylonitrile) binary blends. J Macromol Sci Part B 51(1):22–34
5. Gupta B, Gautam D, Ikram S (2013) Preparation of proton exchange membranes by radiation-induced grafting of alpha methyl styrene–butyl acrylate mixture onto polyetheretherketone (PEEK) films. Polym bull 70(10):2691–2708
6. Halasa AF, Seo KS (2014) Anionic solution copolymerization of α-methylstyrene with conjugated dienes above the ceiling temperature of α-methylstyrene. Eur Polym J 51:80–86
7. Banerjee S, Paira TK, Mandal TK (2013) Control of molecular weight and tacticity in stereospecific living cationic polymerization of α-methylstyrene at 0 °C Using $FeCl_3$-based initiators: effect of tacticity on thermal properties. Macromol Chem Phys 214(12):1332–1344
8. Wang W, Lu W, Goodwin A, Wang H, Yin P, Kang NG, Hong K, Mays JW (2019) Recent advances in thermoplastic elastomers from living polymerizations: macromolecular architectures and supramolecular chemistry. Prog Polym Sci 95:1–31
9. Li Y, Knauss DM (2018) Sequential bulk anionic polymerization of α-methylstyrene and isoprene to form diblock and triblock copolymers. Macromol Chem Phys 219(1):1700449
10. Nogueira RF, Tavares MIB (2001) Carbon-13 NMR study of poly (alpha–methylstyrene). Polym Test 20(4):379–382

11. Chen Q, Liu M, Pan D, Chen S, Shi R, Qi X, Zhang Z, Li B (2018) Effects of n-hexadecane on sphericity of poly-α-methylstyrene shells. Colloid Surface A 554:1–8
12. Shangguan X, Chen S, Ma S, Liu M, Tang C, Yi Y, Zhang Z (2017) Effect of molecular weight on the quality of poly (alpha-methylstyrene) mandrel. J Rheol 2(4):197–203
13. Gubler L, Slaski M, Wallasch F, Wokaun A, Scherer GG (2009) Radiation grafted fuel cell membranes based on co-grafting of α-methylstyrene and methacrylonitrile into a fluoropolymer base film. J Membrane Sci 339(1–2):68–77
14. Hu G, Wang Y, Ma J, Qiu J, Peng J, Li J, Zhai M (2012) A novel amphoteric ion exchange membrane synthesized by radiation-induced grafting α-methylstyrene and N, N-dimethylaminoethyl methacrylate for vanadium redox flow battery application. J Membrane Sci 407:184–192
15. Garrett RW, Hill DJ, Le TT, O'Donnell JH, Pomery PJ (1992) An ESR study of free radicals formed in irradiated poly (alpha-methyl styrene) by gamma-radiation. Radiat Phys Chem 39(2):215–221
16. Sharma VK, Affrossman S, Pethrick RA (1984) Poly (α-methylstyrene) and α-methylstyrene-maleic anhydride copolymer: an electron beam lithographic study. Polymer 25(8):1087–1089
17. Zhang X, Zhang C, Wang Y, Li Y (2010) Synthesis and characterization of symmetrical triblock copolymers containing crystallizable high-trans-1, 4-polybutadiene. Polym bull 65(3):201–213
18. Ziaee F, Ronagh-Baghbani M, Jozaghkar MR (2019) Microstructure characterization of low molecular weight polybutadiene using the chain end groups by nuclear magnetic resonance spectroscopy. Polym Bull 77:2345–2365
19. Britton D, Heatley F, Lovell PA (1998) Chain transfer to polymer in free-radical bulk and emulsion polymerization of vinyl acetate studied by NMR spectroscopy. Macromolecules 31(9):2828–2837
20. Ahmad NM, Heatley F, Britton D, Lovell PA (1999) Chain transfer to polymer in emulsion polymerization. Macromol Sy 143(1):231–241
21. Britton D, Heatley F, Lovell PA (2001) ^{13}C NMR spectroscopy studies of branching and sequence distribution in copolymers of vinyl acetate and n-butyl acrylate prepared by semibatch emulsion copolymerization. Macromolecules 34(4):817–829
22. Ziaee F, Nekoomanesh M, Mobarakeh HS, Arabi H (2008) The effect of temperature on tacticity for bulk thermal polymerization of styrene. E-Polymers. https://doi.org/10.1515/epoly.2008.8.1.466
23. Brownstein S, Bywater S, Worsfold DJ (1961) The proton resonance spectra of poly-α-methylstyrenes. Macromol Chem Phys 48(1):127–134
24. Sakurada Y, Matsumoto M, Imai K, Nishioka A, Kato Y (1963) Proton magnetic resonance spectra of poly-α-methylstyrene. J Polym Sci Pol Lett 1(11):633–639
25. Inoue Y, Nishioka A, Chûjô R (1972) Carbon-13 nuclear magnetic resonance spectroscopy of polystyrene and poly-α-methylstyrene. Macromol Chem Phys 156(1):207–223
26. Parella T, Espinosa JF (2013) Long-range proton–carbon coupling constants: NMR methods and applications. Prog Nucl Mag Res Sp 73:17–55
27. Yazgan I (2020) NMR-based structural characterization of common aromatic poly(amic acid) polymers. Polym Bull 77(3):1191–1203
28. Vögeli B (2014) The nuclear overhauser effect from a quantitative perspective. Prog Nucl Mag Res Sp 78:1–46
29. Elgert KF, Wicke R, Stützel B, Ritter W (1975) On the structure of poly (α-methylstyrene): 13C nmr spectra at 67.88 and at 90.51 MHz. Polymer 16(6):465–467
30. Ziaee F, Salehi MH (2011) Effect of temperature on polystyrene tacticity through para aromatic carbon splitting in 13C NMR spectroscopy. Iran Polym J 20(3):213–221
31. Odian G (2004) Principles of polymerization. Wiley, New York
32. Tonelli AE (2017) From NMR spectra to molecular structures and conformation. stereochemistry and global connectivity: the legacy of ernest L. Eliel 2:161–190
33. Ziaee F, Bouhendi H (2009) NMR study of polyacrylamide tacticity synthesized by precipitated polymerization method. Iran Polym J 18(12):947–956